THE JOURNAL OF PHYSICAL CHEMISTRY A

Article

pubs.acs.org/JPCA

Preferential Formation of the Different Hydrogen Bonds and Their Effects in Tetrahydrofuran and Tetrahydropyran Microhydrated Complexes

Margarita M. Vallejos and Nélida M. Peruchena*

Laboratorio de Estructura Molecular y Propiedades, Área de Química Física, Departamento de Química, Facultad de Ciencias Exactas y Naturales y Agrimensura, Universidad Nacional del Nordeste, Avda. Libertad 5460, (3400) Corrientes, Argentina

Supporting Information

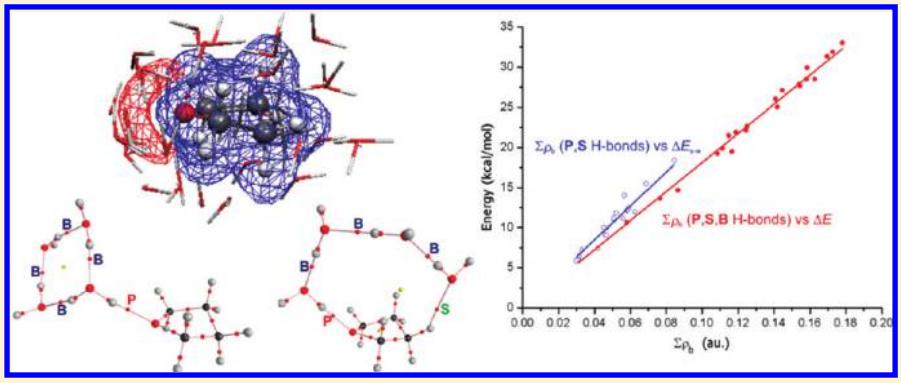

ABSTRACT: The role of cycloether−water (c−w) and water−water (w−w) hydrogen bonds (H-bonds) on the stability of the tetrahydrofuran THF/$(H_2O)_n$ and the tetrahydropyran THP/$(H_2O)_n$ complexes with n = 1−4 was investigated herein using the density functional and ab initio methods and the atoms in molecules theory. Geometry optimizations for these complexes were carried out with various possible initial guess structures. It was revealed that the major contributions of the mono and dihydrated complexes came from c−w H-bonds. A competition between c−w and w−w H-bonds contribution was observed for trihydrated complexes. For most of tetrahydrated complexes, the inter-water H-bonds provided the greatest contribution, whereas the c−w contributions were small but not negligible. It was confirmed that to produce a hydrophobic hydration of cycloethers, the C−H···O_w H-bond should be associated with a network of H-bonds that connects both portions of the solute, through the formation of a bifunctional H-bond. A linear correlation is obtained for the sum of electron density at the bond critical points (ρ_b) with the interaction energy (ΔE) and with the solute−solvent interaction energy (ΔE_{s-w}) of the microhydrated complexes. In addition, a new way to estimate the energetic contribution as well as the preferential formation of the different H-bonds based completely on ρ_b was found. Even more, it allows to differentiate the contribution from c−w interactions in both hydrophilic and hydrophobic contributions, it is therefore a useful tool for studying the hydration of large biomolecules. The analysis of the modifications in the atomic and group properties brought about by successive addition of H_2O molecules allowed to pinpoint the atoms or molecular groups that undergo the greatest changes in electron population and energetic stabilization. It was identified that the remarkable stabilization of the water oxygen atoms is crucial for the stabilization of the complexes.

1. INTRODUCTION

Hydration is a universal phenomenon in nature, many chemical and biological processes occur in aqueous media.[1−6] In the hydration of organic compounds which have polar groups, water molecules interact with them through both hydrophilic and hydrophobic hydration. One of the most important intermolecular interactions that occurs in this type of hydration is the hydrogen bond (H-bond), which has been the aim of a large number of studies within the field of molecular hydration.[7−12]

Several studies have been carried out on hydration of organic compounds employing a large amount of theoretical[13−15] and experimental techniques.[16−18] Vibrational spectroscopy is especially suited for such studies since the strength of H-bond can be easily estimated from the vibrational wavenumber and bond length. In this sense, several works have been reported in which the hydration of soluble molecules shows an increase of the stretch frequency, ν(C−H) (i.e., ethanol/water).[19−22] In these cases, the water molecule interacts simultaneously with the hydroxyl group and with the hydrogen atoms of the methyl group of the ethanol. In the same context, Mizuno and co-workers[23,24] have studied the concentration dependence of ν(C−H)s in IR and 1J(C,H) in NMR for 1,4-dioxane/water and tetrahydrofuran/water mixtures over the

Received: February 14, 2012
Revised: March 19, 2012
Published: March 19, 2012

whole range of concentrations to determine the role of the polar group on the H-bond formation at the hydrophilic and hydrophobic portions. They found out that when the water concentration increases the ν(C−H) stretching modes blue shifts and the absorption intensities of the same modes decrease. Additionally, they have found a slight increase in the chemical shifts of NMR (δCH) with the X_{H_2O} increase. Although molecular interactions in aqueous solutions are much more complex than those in gas phase, Mizuno et al. have associated the blue shifts in the ν(C−H)s, observed for the aqueous solutions, with the same blue shifting H-bonds formed between a proton donor and a water molecule in the gas−phase calculations. They proposed the formation of a "bifunctional hydrogen-bonding hydration complex", in which the water molecule plays the role of a proton donor in conventional O−H···O H-bond, and a proton acceptor in blue shifting C−H···OH_2 H-bond, simultaneously.[23]

A key aspect here is that the majority of organic molecules are chemically heterogeneous with hydrophilic and hydrophobic portions and this heterogeneity is more extensive in many biochemical contexts. This strongly suggests that one must first understand the hydration around simple solutes and the complexes studied here can be regarded as simplified models for the study of the hydrophilic and hydrophobic hydration. In addition, a simple but insightful way to study the hydration phenomenon is through microhydration, that is, the formation of complexes between a few discrete water molecules and the solute.[25] In this approach, the determination of structures and relative energies of microhydrated complexes is still an important challenger because the number of possible aggregates increases rapidly when more water molecules are considered.

Thus, in the present work we have explored the microhydration of tetrahydrofuran (THF) and tetrahydropyran (THP) compounds considering the complexes THF/$(H_2O)_n$ and THP$(H_2O)_n$ (with n = 1−4) to gain insight about which intermolecular interactions, either solute−water (c−w) or water−water (w−w), are dominant and what type of hydrogen bonding patterns are involved in the most stable microhydrated structures of n-size. THF and THP compounds were chosen as convenient models for the hydrophilic and hydrophobic hydration because they are computationally affordable due to their small size and because these cycloethers may induce interesting hydration behavior depending on the competition between hydrophilic and hydrophobic interactions.[16a,26−28] In addition, for the most stable complexes we have carried out a deeper analysis of the atomic properties within the framework of the atoms in molecules (AIM) theory[29,30] to achieve a full understanding of the charge distribution and to pinpoint the atoms or regions that experience changes in their electron population and energy upon the microhydration.

2. METHODS AND CALCULATION DETAILS

2.1. Structures. Numerous starting geometries for microhydrated complexes THF/$(H_2O)_n$ (**nF**) and THP/$(H_2O)_n$ (**nP**) with n = 1−4, have been considered. The initial guess structures were generated systematically using their molecular electrostatic potential (MEP) and the AGOA 2.0 program.[31,32] Then, these structures were optimized at the B3LYP/6-31+G(d,p) level. After this, all resulting structures were reoptimized at the B3LYP/6-311+G(d,p) level. Moreover, a tight optimization convergence criterion has been used for some specific complexes. Density functional theory (DFT) has been shown in many investigations to be useful for describing hydrogen-bonded systems.[33,34] In particular, the B3LYP method, which combines Beckès three-parameter nonlocal hybrid exchange potential[35] with the nonlocal correlation functional of Lee, Yang, and Parr,[36] gave a good description of the structural parameter changes issued from the H-bond interactions for the study of such systems.[14] Vibrational frequencies of the reoptimized structures were calculated to ensure that they indeed represent local minima on the potential energy surfaces, that is, no imaginary frequencies are present.

2.2. Energetic Parameters. The interaction energy (ΔE) of each complex was calculated as the difference between the energy of the complex and the sum of energies of the isolated monomers. This energy can be expressed as

$$\Delta E = E_{\text{cycloether}/(H_2O)_n} - (E_{\text{cycloether}} + nE_{H_2O})$$

where $E_{\text{cycloether}/(H_2O)n}$, refers to energy of microhydrated complex, and $E_{\text{cycloether}}$ and E_{H_2O} refer to the energy of the isolated cycloether and H_2O molecule, respectively. ΔE measures the total interaction energy in the microhydrated complex of n-size; and it is considered as an estimation of the strength of c−w and w−w H-bonds in microhydrated complexes. To estimate interaction energy between the cycloether and the water subcluster $(H_2O)_n$, we used the solute−solvent interaction energy (ΔE_{s-w}), which can be defined as[37]

$$\Delta E_{s-w} = E_{\text{cycloether}/(H_2O)_n} - (E^{c}_{\text{cycloether}} + E^{c}_{nH_2O})$$

where $E^{c}_{\text{cycloether}}$, $E^{c}_{nH_2O}$, indicate the cycloether and the water subcluster energies, both of them calculated on the complex geometry. This definition suggests that the ΔE_{s-w} takes into accounts the net interaction between c−w disregarding the inter-water interactions.

It is important to consider that a balance between solute−water and w−w interactions determines the structure of a hydrated organic complex. In this regard, Geronimo et al.[38] have recently introduced a ratio to measure semi−quantitatively the competitive formation of solute−water and inter-water H-bonds network in hydrogen-bonded hydrated complexes defined as

$$\mathcal{H} = \frac{\Delta E - \Delta E_{s-w} + E_{def-c} + E_{def-w}}{\Delta E}$$

where E_{def-c} and E_{def-w} are deformation energies (one per subclusters), which correspond to the energy difference between the frozen geometry within the microhydrated complexes and the absolute geometry minimum for each monomer. The E_{def-w} for each complex is the sum of the individual deformation energy of the n water in it. According to these authors,[38] a $\mathcal{H}$ value higher than 0.5 indicates a preferential formation of inter-waters H-bonds over water−solute H-bonds.

Single-point energy calculations of each optimized structure were carried out to better estimate the hydrogen bonding strengths by applying second order Møller−Plesset perturbation theory (MP2)[39] adopting the 6-311++G(d,p) set of basis function. In addition, the reliability of the MP2 energy ordering was calculated by comparing it with that obtained in single point CCSD(T)/6-311+G(d,p) calculations carried out on MP2/6-311+G(d,p) optimized geometries, for the different

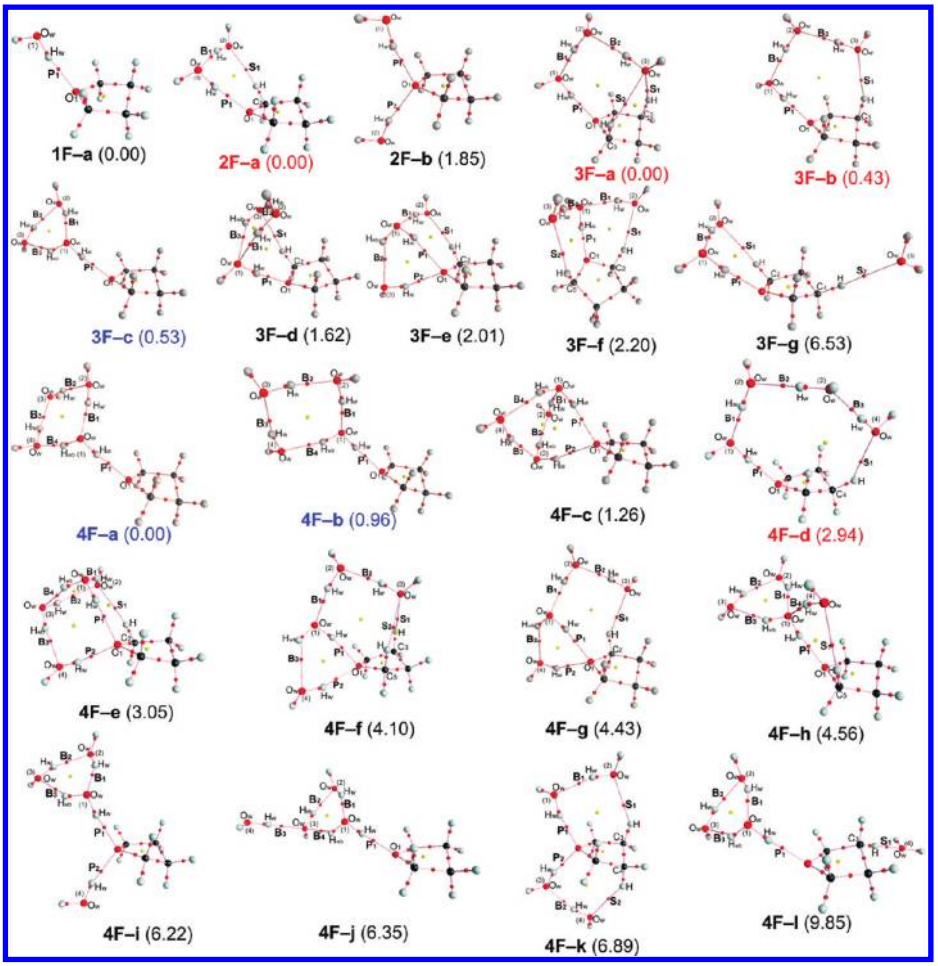

Figure 1. Molecular graphs for **nF** complexes (n = 1−4) along with the corresponding relative energy in kcal/mol (the energy of any structure minus the energy of structure **nF−a**). Big circles correspond to attractors attributed to nuclei positions of H (gray), C (black), and O (red); lines connecting the nuclei are the bond paths. Small circle are attributed to bond critical points BCP (red) and ring critical points RCP (yellow). The BCPs corresponding to primary, secondary, and inter-water H-bonds are denoted as **P**, **S**, and **B**, respectively. The complexes with **HT** and **CL** patterns are labeled in red and blue fonts, respectively.

structures of microhydrated complexes, as suitable model systems. The calculated energies were corrected for the basis set superposition error (BSSE), using counterpoise method.[40]

2.3. AIM Analysis. Electron density was obtained using the AIM2000 program.[41] The values of electron density (ρ_b) and its Laplacian ($\nabla^2\rho_b$) at the bond critical points (BCPs) were used to characterize the H-bonding interactions. The atomic properties have also been evaluated within the AIM methodology. Calculation of the atomic properties has been carried out by integration within the atomic basins. The accuracy of the integrated properties was tested taking into account that the summations of atomic electron population, $N(\Omega)$, and atomic energy, $E(\Omega)$, values for each molecule reproduce total electron populations and electronic molecular energies within 0.001 au and 1 kcal/mol, respectively. In addition, all the integrated atomic properties were obtained with values of $|L(\Omega)|$ less than 4×10^{-4} for the carbon and oxygen atoms and less than 10^{-5} for the hydrogen atom as it is specified in the literature.[42] All electronic structures were obtained using the Gaussian 03 suite of programs.[43]

3. RESULTS AND DISCUSSION

3.1. Structural and Electron Charge Density Analysis. Molecular graphs of the **nF−x** and **nP−x** complexes, wherein **x** is an index that categorizes the complexes in increasing energy (within such class), are displayed in Figures 1 and 2, respectively. Optimized structures of the microhydrated complexes are displayed in Figures S1 and S2, respectively, and their optimized parameters as the H-bond distance (rH···X) the variation of the X−H bond distance upon the complexation (ΔrX−H) and bond angle ($\angle$XHY) along with the electron topological properties, as electron charge density (ρ_b) and its Laplacian ($\nabla^2\rho_b$) evaluated at the H···Y BCP, are listed in Tables S1 and S2 of the Supporting Information. From Figures 1 and 2, three types of H-bonds can be differentiated in microhydrated complexes: (i) O_w−H_w···O_1 primary H-bond (denoted by **P**) formed between the oxygen heteroatom of THF or THP and de hydroxyl group of a water molecule; (ii) C−H···O_w secondary H-bond (denoted by **S**) between the hydrogen atom of CH_2 group of the cycloether and the oxygen atom of water molecule; and (iii) O_w−H_w···H_w water bridge H-bond (denoted by **B**). Thus, **P** H-bond is related to hydration of the hydrophilic portion of cycloether while **S** H-bond is involved in hydration of the hydrophobic portion of cycloether. The presence of **P**, **S**, and **B** H-bonds in **nF** and **nP** complexes is revealed by the existence of BCPs in the molecular graphs. On the other hand, the results obtained show a good agreement

dx.doi.org/10.1021/jp301498n | J. Phys. Chem. A 2012, 116, 4199−4210

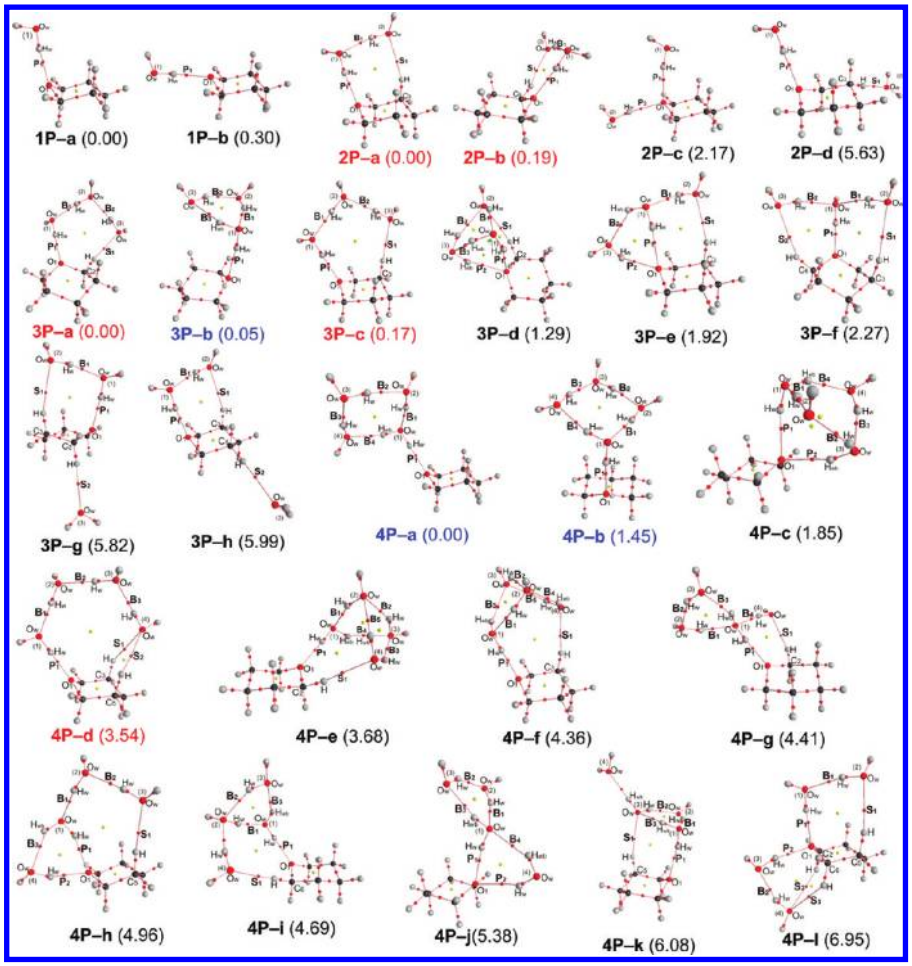

Figure 2. Molecular graphs for **nP** complexes (n = 1−4) along with the corresponding relative energy in kcal/mol (the energy of any structure minus the energy of structure **nP−a**). Big circles correspond to attractors attributed to nuclei positions of H (gray), C (black), and O (red); lines connecting the nuclei are the bond paths. Small circle are attributed to bond critical points BCP (red), ring critical points RCP (yellow) and cage critical points CCP (green). The BCPs corresponding to primary, secondary, and interwater H-bonds are denoted as **P**, **S**, and **B**, respectively. The complexes with **HT** and **CL** patterns are labeled in red and blue fonts, respectively.

between DFT and ab initio geometries (see Tables S1 and S2 of the Supporting Information).

Cycloether Monohydrated Complexes. One and two structures of minima energy were found for monohydrated complex of THF (**1F−a**) and THP (**1P−a,b**; see Figures 1 and 2, respectively). In these complexes, only one $\mathbf{P_1}$ H-bond was involved, whose bond distance is of ∼1.8 Å and bond angle is of ∼170°. Furthermore, this interaction is characterized by the existence of a BCP between H_{w1} atom and the O_1 heteroatom and the values of ρ_b and $\nabla^2\rho_b$ at the $\mathbf{P_1}$ H-bond BCPs fall within the proposed range for the H-bonds.[44] (see Tables S1 and S2 in the Supporting Information). The calculated geometry of the **1F−a** complex agrees with the structures of the THF/H_2O calculated by Sahu and co-workers[45] and Mizuno et al.[24] in their ab initio and DFT studies.

Cycloether Dihydrated Complexes. Two minima energy structures were obtained for the **2F** complexes and four for the **2P** complexes which are depicted in Figures 1 and 2, respectively. The most stable dihydrated structures correspond to **2F−a**, and **2P−(a,b)** complexes in which **P**, **B**, and **S** H-bonds are formed. In these complexes, water molecules behave as both proton donor and proton acceptor simultaneously, forming a bifunctional H-bond where the hydrophilic ("head") and hydrophobic ("tail") portions of cycloether are connected through a bridge formed by two water molecules. (This is: $O_{(head)}\cdots(H_2O)_{n(water\ bridge)}\cdots H-C_{(tail)}$ or in a more universal form "head−water bridge−tail"). We will refer to this type of hydrogen bonding pattern as **HT** pattern, hereafter. In **2F−a**, and **2P−(a,b)** complexes the $\mathbf{P_1}$ H-bond is enhanced with respect to either **1F** and **1P** complexes, because the $H_{w1}\cdots O_1$ bond distance decreases about 0.10 Å, and the values of ρ_b as well as $\nabla^2\rho_b$ are larger at the $\mathbf{P_1}$ H-bond BCP than in the monohydrated complexes (see Tables S1 and S2 in Supporting Information). This strengthening of the $\mathbf{P_1}$ H-bond in dihydrated complexes is produced as a consequence of the characteristic cooperative effect in bifuncional H-bond, $(>O_1\cdots H_{w1}-O_{w1}\cdots H_{w2}-O_{w2}\cdots H-C)$.[46] In the case of the **S** H-bond, it shows a longer bond distance (∼2.50 Å) and lower values of ρ_b as well as $\nabla^2\rho_b$, which denote the weakness of this interaction involved in the hydrophobic hydration. For the THF/$(H_2O)_2$ complex, Mizuno et al.[24] found three structures using DFT and MP2 methods with large basis sets and as in **2F−a** complex, a bifunctional H-bond was involved in the most stable of those structures.

In **2F−b** and **2P−c** complexes, whose relative energies are 1.85 and 2.17 kcal/mol, respectively, the heteroatom acts as double proton acceptor forming two **P** H-bonds ($\mathbf{P_1}$ and $\mathbf{P_2}$ H-bonds), and their bond distances are longer than those in the

dx.doi.org/10.1021/jp301498n | J. Phys. Chem. A 2012, 116, 4199−4210

Table 1. Energetic Parameters and Percentual Contribution of the Different H-Bonds Based on the Electron Charge Density for Selected nF and nP Complexes (n = 1−4)[a]

complexes	ΔE	ΔE_{s-w}	$\mathcal{H}$	P%	S%	B%	(P + S)%
1F−a	−5.85 (−5.59)	−6.12		100.0	0.0	0.0	100.0
2F−a	−12.65 (−12.52)	−9.30	0.33	48.2	11.9	39.9	60.1
3F−a	−20.67 (−19.87)	−11.61	0.50	32.7	12.1	55.2	44.8
3F−c	−20.10 (−19.30)	−7.47	0.69	27.6	0.0	72.4	27.6
4F−a	−30.42	−7.72	0.82	17.3	0.0	82.7	17.3
4F−d	−27.48	−11.28	0.66	26.3	6.6	67.1	32.9
1P−a	−5.67 (−5.41)	−5.98		100.0	0.0	0.0	100.0
2P−a	−12.32 (−11.82)	−8.96	0.34	48.3	11.3	40.4	59.6
3P−a	−19.31 (−18.89)	−10.21	0.54	31.5	10.1	58.4	41.6
3P−b	−19.26 (−18.90)	−6.77	0.71	26.9	0.0	73.1	26.9
4P−a	−29.59	−7.92	0.81	17.2	0.0	82.8	17.2
4P−d	−26.04	−10.86	0.65	24.0	8.9	67.1	32.9

[a]The energies are given in kcal/mol; $\mathcal{H}$ ratio is dimensionless. All symbols are explained in the text. See Figures 1 and 2 to identify the complexes. Data in italics refer to values calculated at CCSD(T)/6-311+G(d,p)//MP2/6-311+G(d,p) level. This information for the remaining complexes is summarized in Table S3 of the Supporting Information.

complex that exhibits **HT** pattern, as well as in the monohydrated complexes. This result agrees with the IR spectroscopic studies[27,47] of the THF in aqueous solution at different concentrations through which it was concluded that the ether oxygen is coordinated by only a single water molecule at X_{H_2O} = 0.78, and that the anticooperative effect of H-bonds occurs when two water molecules interact with lone pairs of the heteroatom. Therefore, it is assumed that in aqueous solution the formation of **2F−b** and **2P−c** complexes will be less probable. The least stable dihydrated complex is the **2P−d** whose relative energy is 5.63 kcal/mol, in this complex there is a $\mathbf{P}_1$ H-bond and a simple **S** H-bond. Unlike the most stable complexes (**2P−(a,b)**), these H-bonds are not connected by an inter-water H-bond.

Cycloether Trihydrated Complexes. As expected, the number of possible structures increases with the raise in the number of water molecules. In fact, seven (**a−g**) and eight (**a−h**) minima energy structures were found for **3F** and **3P** complexes, respectively (see Figures 1 and 2). The first three lower energy complexes **3F−(a−c)** and **3P−(a−c)** are very close in energy (E_{rel} < 1 kcal/mol). However, it is noticeable that, from these energetically favorable hydration structures, two different hydrogen bonding patterns are shown. One of them is represented by the **3F−(a,b)** and **3P−(a,c)** complexes, and these show an **HT** pattern. For the other most stable trihydrated complexes (**3F−c** and **3P−b**), the $H_2O_{(1)}$ molecule is attached to the heteroatom through a simple $\mathbf{P}_1$ H-bond and the three water molecules are bonded between them forming a closed-loop (**CL**) H-bonded structure. And we will refer to this type of H-bonds arrangement as **CL** pattern, hereafter.

The relative energy for **3F−(d−f)** and **3P−(e,f)** complexes falls within the range of 1.3 to 2.3 kcal/mol, while for the **3F−g** and **3P−(g,h)** complexes it is higher than 5.5 kcal/mol. In the **3F−e** and **3P−e** complexes, the heteroatom acts as a double proton acceptor interacting with two water molecules simultaneously through the $\mathbf{P}_1$ and $\mathbf{P}_2$ H-bonds. As we have mentioned above, due to the anticooperative effect in this kind of H-bonding arrangement, these H-bonds have the highest bond distances. In **3F−g** and **3P−(g,h)** complexes, two water molecules, $H_2O_{(1,2)}$, adopt a orientation similar to those in the lowest energy dihydrated complexes (**2F−a** and **2P−(a,b)**). However, these hydration structures are the least stable because the third water molecule, $H_2O_{(3)}$, is involved in a simple **S** H-bond ($C-H\cdots O_{w(3)}$). Thus, it should be noted that when the water molecules are bonded with the hydrogen atoms of the hydrophobic methylen group through a simple **S** H-bond which marks a common feature in the least stable microhydrated complexes. These findings constitute the first hint that $C-H\cdots O_w$ H-bond contributes scarcely to the stabilization of the complexes when it appears in an isolated form. In other words, the hydrophobic hydration is most favorable when a bifunctional H-bond, (i.e., $>O_1\cdots(H_w-O_w)_n\cdots H-C$) is formed.

Cycloether Tetrahydrated Complexes. A total of 12 different structures for both **4F** and **4P** complexes which are displayed in Figures 1 (**4F−(a−l)**) and 2 (**4P−(a−l)**), respectively, were obtained. From these figures it can be seen that the relative energy of **4F−(a−c)** and **4P−(a−c)** complexes is lower than 1.3 and 1.9 kcal/mol, respectively. The **4F−(a,b)** and **4P−(a,b)** complexes show a **CL** pattern, wherein the water molecules are self-associated through four **B** H-bonds, forming a four-member ring, and one of the water molecules is connected to the O_1 heteroatom through a $\mathbf{P}_1$ H-bond. In both **4F−(a,b)** complexes, the $\mathbf{P}_1$ H-bond distance is longer than the one in the **3F−a** complex by 0.12 Å, and in the **4P−(a,b)** complexes this bond distance is longer than the one in the **3P−a** complexes, too, by 0.09 and 0.12 Å, respectively. However, it is to note that in the above complexes, the $\mathbf{B}_{1-4}$ H-bonds are the strongest intermolecular H-bonds involving the shortest bond distances and the largest values of ρ_b as well as of $\nabla^2\rho_b$ (see Tables S1 and S2 of the Supporting Information). In fact, more cooperativity deriving from the multiple **B** H-bonds formed between the four molecules is helpful in the strengthening of these H-bonds. These results agree with those reported by other authors,[48] wherein the four-water ring constitutes a structural motif often found in microhydration, as an energetically favorable H-bonding pattern.

In **4F−c** and **4P−c** complexes, two water molecules are attached to the O_1 heteroatom forming two **P** H-bonds. These H-bonds have relatively long bond distances (∼2.00 Å) and their bond angles values are between 159 and 163°. As it was above referenced,[27] this H-bonding arrangement type is unfavorable due to the anticooperative effect. The **4F−d** and **4P−d** complexes show an **HT** pattern and they are less stable than **4F−a** and **4P−a** complexes by 2.94 and 3.54 kcal/mol, respectively. The $\mathbf{P}_1$ H-bond distance in these complexes, is the shortest of tetrahydrated complexes series (1.723 Å in the **4F−**

d complex and 1.745 Å in **4P−d** complex) and it has a bond angle of ∼177°. Thus, it can be assumed that the **HT** pattern leads to the most strengthened $\mathbf{P}_1$ H-bond as a consequence of the cooperativity effect that exists among multiple H-bonds. However, this type of pattern is not involved in the most stable tetrahydrated structure, because there is an enhancement of the **B** H-bond attributed to the cooperative effect as well.

For the **4F−(e−k)** complexes, the relative energy varies between 4.0 and 7.0 kcal/mol, while for the **4F−l** complexes, it increases to 9.9 kcal/mol. In the former complexes, the water molecules tend to be self-associated, forming three or four **B** H-bonds. Here again, in the least stable complex (**4F−l**), one of the water molecules, $H_2O_{(4)}$, acts only as a proton donor forming a simple **S** H-bond. Throughout these observations and taking into account previous results about the structures of the least stable microhydrated complexes of *n*-size, it can be confirmed that to produce a hydrophobic hydration of cycloethers, the **S** H-bond should be associated with a network of H-bonds that connects both portions of the solute, that is to say, through the formation of a bifunctional H-bond. Likewise, the structures of **4F−(e−k)**, the **4P−(e−l)** complexes whose relative energy varies between 3.7 and 7.0 kcal/mol, show different arrangements of water molecules self-association wherein between three and five **B** H-bonds are involved (see Figure 2). Thus, this distinctive arrangement of water molecules suggests that the cooperativity of the H-bonds between water molecules may be a dominant phenomenon when $n > 4$.

On the other hand, it is interesting and significant to know, first, how much the c−w and w−w H-bonds contribute on the stability of microhydrated complexes; second, what the key contributions are and how these are modified when *n* increases. These questions can be answered through the energetic analysis considering the energetic parameters defined in the methodology section and in the analysis of AIM results.

3.2. Total Interaction Energy and Solute−Solvent Interaction Energy. The calculated ΔE, ΔE_{s-w}, and $\mathcal{H}$ ratio previously defined in the methodology section for selected microhydrated complexes are listed in Table 1. As it can be seen from this table, the ΔE of the complexes increases with the raise in the number of water molecules, accounting for c−w as well as w−w interactions. The ΔE calculated value for the **1F−a** complex (−5.85 kcal mol) is slightly higher than it is for **1P−(a,b)** complexes (−5.67 and −5.38 kcal/mol) in agreement with the $\mathbf{P}_1$ H-bond distance. As it is expected, $\Delta E \sim \Delta E_{s-w}$ because in these complexes only a single intermolecular interaction ($\mathbf{P}_1$ H-bond) occurs. In the most stable dihydrated complexes **2F−a** and **2P−(a,b)**, (with **HT** pattern) the $\Delta E > \Delta E_{s-w}$, giving as a consequence the values of $\mathcal{H}$ ratio close to 0.3. These values indicate the dominant contribution of the c−w interactions compared to w−w interactions on the ΔE. For **2F−b** and **2P−(c,d)** complexes, where **B** H-bonds do not form, the values of $\mathcal{H}$ ratio are very small (0.1); therefore, the energetic contribution to the interaction energy of the complexes comes mainly from c−w interaction and, in particular, from the $\mathbf{P}_1$ H-bond (see Table S3 of the Supporting Information).

When *n* increases in the systems, the $\mathcal{H}$ ratio increases as well, indicating that the w−w interactions acquire gradually more importance in the stabilization of the microhydrated structures. For **3F−(a−c)** and **3P−(a−c)** complexes, ΔE differs very slightly from one another, as it was previously indicated through their relative energy. However, it should be noted that among these complexes there is a difference in their respective ΔE_{s-w}, reflected in the values of the $\mathcal{H}$ ratio. In this sense, for the **3F−(a,b)** and **3P−(a,c)** complexes, the $\mathcal{H}$ ratio is 0.5 indicating a similar contribution of c−w and w−w H-bonds to their ΔE. On the other hand, for the **3F−c** and **3P−b** complexes with **CL** pattern, the $\mathcal{H}$ ratio takes value ∼0.7. These results do indicate that for trihydrated cycloether there are two energetically competitive structures involved, either **HT** or **CL** pattern. In all the rest of trihydrated complexes, **3F−(d−g)** and **3P−(e−h)**, the $\mathcal{H}$ ratio is systematically lower than 0.5 indicating a slight prevalence of the c−w interactions over those that occur between the water molecules (see Table S3 of the Supporting Information). For **4F** and **4P** complexes, the ΔE acquire higher values ranging between −30.42 and −20.56 kcal/mol, and between −29.59 and −22.63 kcal/mol, respectively. In contraposition, for most of these complexes, the values calculated for ΔE_{s-w} are comparatively low and, as a consequence, their $\mathcal{H}$ ratio are higher than 0.5. Thus, the w−w interactions, that is, the **B** H-bonds, become the main contribution to the ΔE of tetrahydrated complexes. Additionally, it is to note that for the most stable tetrahydrated complexes (**4F−a−c** and **4P−a−c**) the $\mathcal{H}$ ratio reached considerable high values (∼0.8). It is to be noted that the energies obtained at the CCSD(T)/6-311+G(d,p) level on MP2/6-311+G(d,p)-optimized geometries are in the same order as predicted by MP2 results.

Moreover, in several previous works it has been found that the sum of the ρ_b values at the intermolecular H-bonds BCPs ($\Sigma\rho_b$) in complexes is a measure of the H-bonds strength and that it increases linearly with ΔE.[44,49−51] Figure 3 shows a good

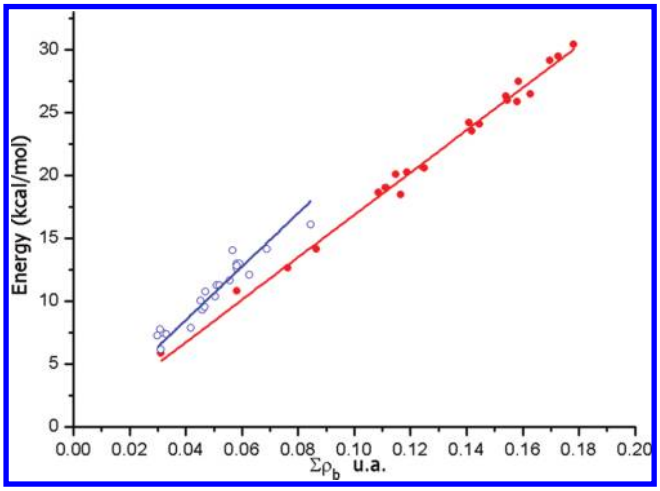

Figure 3. Relationship between absolute values of ΔE and $\Sigma\rho_b$ at all H-bond BCPs (red line), along with the relationship between absolute values of ΔE_{s-w} and $\Sigma\rho_b$ at the **P** and **B** H-bonds BCPs (blue line), for **Fn** complexes.

linear correlation between $\Sigma\rho_b$ at all H-bonds (**P**, **S**, **B**) and ΔE for all the microhydrated complexes. The linear regression analysis yields

$$-\Delta E = 168.66\Sigma\rho_b(\mathbf{P}, \mathbf{S}, \mathbf{B}\ \text{H-bonds})$$

$$R^2 = 0.999, \quad \text{for } \mathbf{nF} \text{ complexes and}$$

$$-\Delta E = 163.91\Sigma\rho_b(\mathbf{P}, \mathbf{S}, \mathbf{B}\ \text{H-bonds})$$

$$R^2 = 0.999, \quad \text{for } \mathbf{nP} \text{ complexes}$$

dx.doi.org/10.1021/jp301498n | J. Phys. Chem. A 2012, 116, 4199−4210

Table 2. Fundamental Vibrational Frequencies of the Stretching Modes of the Monomers (in Italics) and Their Shift upon the Formation of Selected nF and nP Complexes[a]

systems	$\nu_s(O_w-H_w)$	$\nu_s[C_{(2,5)}-H]$	$\nu_{as}[C_{(3,4)}-H]$	systems	$\nu_s(O_w-H_w)$	$\nu_s[C_{(2,6)}-H]$	$\nu_{as}[C_{(3,4,5)}-H]$
THF		*2872.2*	*2975.7*	THP		*2835.2*	*2941.9*
1F−a	−191	14.1	6.0	**1P−a**	−177	23.4	5.9
2F−a	−320	21.8	9.9	**2P−a**	−307	26.2	10.1
3F−a	−405	19.6	13.0	**3P−a**	−356	23.5	7.0
3F−c	−373	20.2	6.0	**3P−b**	−356	23.6	5.3
4F−a	−514	20.0	5.4	**4P−a**	−506	22.8	4.9
4F−d	−416	11.5	25.7	**4P−d**	−375	19.6	14.9

[a]The values are given in cm^{-1}. A scaling factor of 0.96 is applied to account for the anharmonic nature of vibration. For water molecule ν_s = 3663 cm^{-1}. Symbols are explained in the text.

This figure also shows the relationship between $\Sigma\rho_b$, evaluated at the **P** and **S** H-bonds BCPs for **nF** complexes and the ΔE_{s-w}. The graph of these relationships obtained for the **nF** complexes is very similar to **nP** complexes but it is not shown here. As it has been previously defined, ΔE_{s-w} takes into account the net interactions between the solute and water molecules, in other words, ΔE_{s-w} assesses the **P** and **S** H-bonds formed between water molecules and hydrophilic and hydrophobic portions of cycloether. Accordingly, a good linear correlation between the $\Sigma\rho_b$ at these H-bonds BCPs and the ΔE_{s-w} is obtained. For this case the equations of linear regression are:

$$-\Delta E_{s-w} = 212.33 \sum \rho_b(\mathbf{P}, \mathbf{S}\text{ H-bonds})$$

$$R^2 = 0.994, \text{ for } \mathbf{nF} \text{ complexes and}$$

$$-\Delta E_{s-w} = 202.59 \sum \rho_b(\mathbf{P}, \mathbf{S}\text{ H-bonds})$$

$$R^2 = 0.994, \text{ for } \mathbf{nP} \text{ complexes}$$

On the basis of the above obtained linear correlations and considering that ρ_b gives an easy indication of H-bond strength, we propose to estimate the different types of H-bond (**P**, **S**, and **B**) contributions to the stability of a complex as the percentage of $\Sigma\rho_b$ at each **P**, **S**, or **B** H-bond BCP compared to $\Sigma\rho_b$ at all H-bond BCPs. The *percentual contribution* of the **P** (*P*%), **S** (*S* %), and **B** (*B*%) H-bonds obtained for **nP** and **nF** complexes are shown in Tables 1. The values of the sum of *S*% and *P*% contributions ((*P* + *S*)%), which correspond to the net contribution of c−w interactions are also included in this table. Overall, the values of the *B*% agree with the values calculated for the $\mathcal{H}$ ratio because both parameters evaluate the contribution of the w−w interaction on the stability of the complexes. Therefore, similar results on c−w and w−w contributions are obtained from the analysis of both parameters ($\mathcal{H}$ ratio and percentual contributions). In addition, through the analysis of the different types of H-bond contributions, it can be seen that, although the **S** H-bond is the weakest, the contribution of this interaction is not negligible. In this sense, for complexes with **HT** pattern *S*% takes values of 9 and 12%, and for less stable tri- and tetrahydrated complexes, this contribution reaches considerable values (see Table S3 of the Supporting Information).

3.3. Vibrational Frequencies. As it has been discussed in the above section, the microhydrated complexes are stabilized by the intermolecular H-bond. As a consequence of these intermolecular interactions, it is expected that the vibrational modes of cycloether and water molecules units in the microhydrated complexes are modified compared to those of isolated monomers. In Table 2 the vibrational frequency shift of $\nu_s(O_w-H_w)$ mode in selected complexes respect to it in isolated water molecule, is shown. In the same table the calculated scaled vibrational frequencies for the most relevant stretching modes of THF and THP along with the shift of these frequencies upon the formation of the selected **nF** and **nP** complexes are also included. As it can be seen in **nF** and **nP** complexes the $\nu_s(O_w-H_w)$ stretching frequency experiences a red shift with respect to that in the free water molecule. The calculated $\nu_s(O_w-H_w)$ red shifts for the **nF** and **nP** complexes vary from −190 to −515 cm^{-1} and from −170 to −505 cm^{-1}, respectively. In addition, it is noteworthy that the red shifting increases going from mono-, di-, tri-, and tetrahydrated complexes due to the cooperative effect, in agreement with the geometrical, energetic, and topological parameters analyzed. For THF in aqueous solution, Mizuno et al.[24] observed a red shift of the ν(O−D) with increasing X_{H_2O}, and they attributed it to an increase in the H-bonding strength of the water in [THF−water−HDO]. However, it should be noted that the $\nu_s(O_w-H_w)$ red shifting in **3F−a** and **3P−a** complexes with **HT** pattern, is similar to that in **3F−c** and **3P−b** complexes with **CL** pattern, respectively. In contrast, the tetrahydrated complexes with **HT** (**4F−d** and **4P−d**) and **CL** (**4F−a** and **4P−a**) H-bonding pattern show dissimilitude in the magnitude of the $\nu_s(O_w-H_w)$ red shift.

On the other hand, most of ν(C−H) modes in the microhydrated complexes get blue-shifted with respect to those in isolated cycloethers. For the THF and their microhydrated complexes, the $\nu_s[C_{(2,5)}-H]$ and $\nu_{as}[C_{(3,4)}-H]$ modes refer to two symmetric and antisymetric modes of groups C_2-H and C_5-H, and C_3-H and C_4-H groups, respectively, which are coupled to each other to become two synchronized modes. Similarly, for the THP and their microhydrated complexes the vibracional frequencies are indicated as $\nu_s[C_{(2,6)}-H]$ and $\nu_{as}[C_{(3,4,5)}-H]$. For **1F−a** and **2F−a** complexes, the calculated blue shifts of the $\nu_s[C_{(2,5)}-H]$ mode are 14.1 and 21.8 cm^{-1}, respectively, and for **3F−a**,**b** and **4F−a** complexes is about 20 cm^{-1}. These values agree with the corresponding experimental values.[24] However, a small blue shift (11.5 cm^{-1}) is observed in the $\nu_s[C_{(2,5)}-H]$ for the **4F−d** complex. Interestingly, although the $C_{(2,5)}-H$ bonds are not themselves directly involved in the **S** H-bond in all complexes, their modes show a blue shift.

The blue shift of the $\nu_{as}[C_{(3,4)}-H]$ mode in **1F−a** complex is 6 cm^{-1}, and it is similar to those for the complexes with **CL** H-bonding pattern (**3F−c** and **4F−a** complexes). In contrast, larger blue shifts are observed for the same stretching frequency in **nF** complexes with **HT** pattern (9.9, 13.0, and 35.7 cm^{-1} for **2F−a**, **3F−a**, and **4F−d** complexes, respectively). These results may be a consequence of the **S** H-bond formation wherein the

dx.doi.org/10.1021/jp301498n | J. Phys. Chem. A 2012, 116, 4199−4210

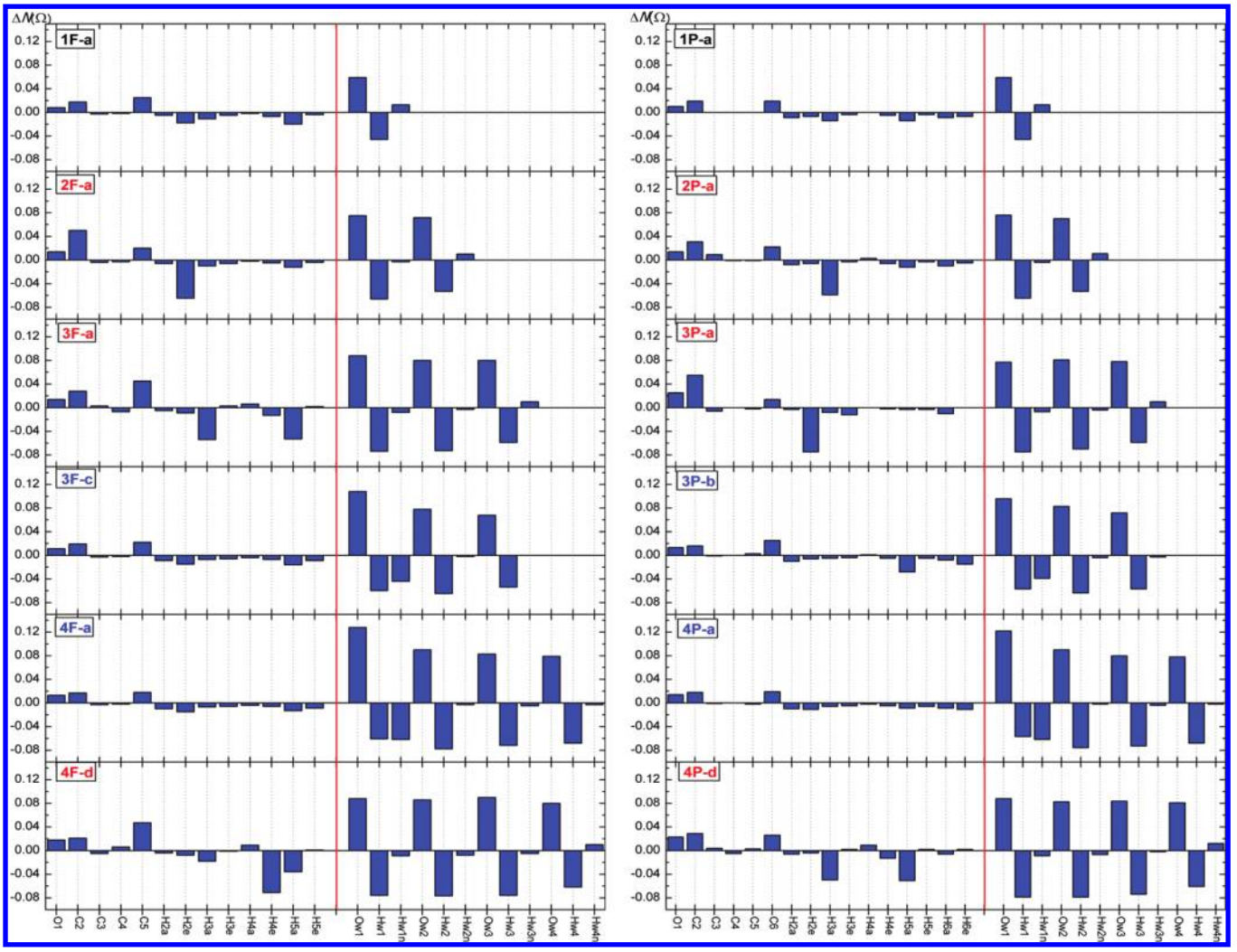

Figure 4. Variation of electron population for all atoms of the selected **nF** (left) and **nP** (right) complexes, in au. The red vertical line separates each bar graph into two regions: the one on the left corresponds to the cycloether atoms (THF and THP) and the other one corresponds to the water molecules atoms. $\Delta N(\Omega) < 0$ and $\Delta N(\Omega) > 0$ indicate that the atom loses and gains electron population upon the complexation, respectively. The complexes with **HT** and **CL** patterns are labeled in red and blue fonts, respectively. See Figures 1 and 2 to identify the complexes and atoms label. In the case of H_{1-4wn} atoms, it indicates the hydrogen atom nonbonding in the H-bond except for complexes **3F−c**, **4F−a**, **3P−b**, and **4P−a**, where both hydrogen atoms of $H_2O_{(1)}$ form an H-bond.

C−H covalent bonds are directly involved. The shift of the calculated $\nu_s[C_{(2,5)}-H]$ and $\nu_{as}[C_{(3,4)}-H]$ vibrational frequencies for the most stable complexes agree with the experimentally observed values in aqueous solution.[24] However, the calculated IR spectrum of complex **4F−d** is slightly different from the IR experimental, in accordance with its lower stability, and thus, these structures might be less favorable in THF in aqueous solution.

As in the C−H stretching modes in **nF** complexes, the frequency of the $\nu_s[C_{(2,6)}-H]$ mode shows a blue shift for **nP** complexes. In **1P−a** and **2P−a** complexes, the calculated blue shift is 23.4 and 26.6 cm^{-1}, respectively, and for the **3P−(a,b)** and **4P−a** complexes it is ∼23 cm^{-1}. The aforementioned results and explanation of the vibrational frecuencies of the **nF** complexes can also be applied to the discussion of the **nP** complexes. However, because there is no experimental evidence for the vibrational spectra of the THP in aqueous solution at present, we believe that these values may be helpful in providing future experimental work. Nevertheless, it should be noted that the experimental spectra will have a mixture of these spectral features due to the response of several energetically comparable structures of complexes with same size.

3.4. Integrated Atomic and Molecular Group Properties. The integration of the properties within the atomic basins provides a tool for analyzing the variation of the total atomic energy, $E(\Omega)$, the atomic net charge, $q(\Omega)$, and the atomic electron population, $N(\Omega)$, associated with microhydration.[30,52,53] Similarly, it is significant for us to analyze the change of properties in "molecular groups" defined as two or more atoms bound together "as a single unit" and forming part of a molecule or of a supramolecule. This analysis aims to pinpoint the atoms or molecular groups that undergo the greatest changes in electron population and energetic stabilization, when the number of water molecules is increased. The changes (ΔP) were calculated subtracting the property value either of the atom $(P(\Omega))$ or of the molecular group $(\Sigma P(\Omega))$ in the isolated monomer to the value of the corresponding property in the microhydrated complex.

Atomic Charge and Electron Population Changes upon the Complexation. Figure 4 displays the atomic population

dx.doi.org/10.1021/jp301498n | J. Phys. Chem. A 2012, 116, 4199−4210

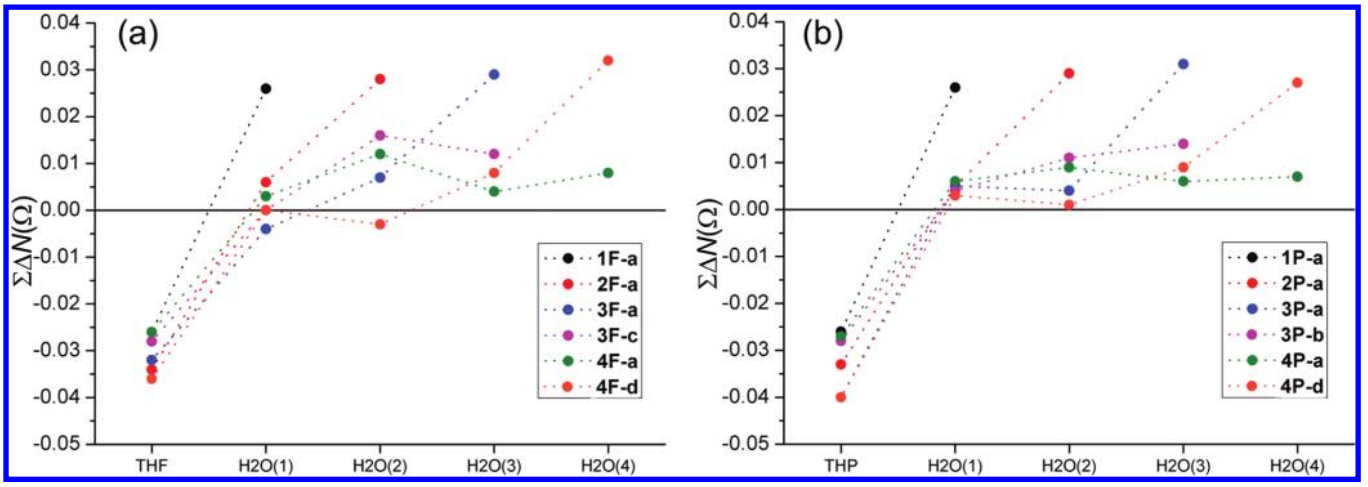

Figure 5. Change in electron population summed up into groups, $\sum\Delta N(\Omega)$, (in au) for selected (a) **nP** and (b) **nF** complexes.

changes, $\Delta N(\Omega)$, on all atoms and Figure 5 shows the change in $N(\Omega)$ summed up into molecular groups, ($\sum\Delta N(\Omega)$), for selected **nP** and **nF** complexes. The atomic net charge, $q(\Omega)$, calculated for selected atoms, are in Tables S4 and S5 of the Supporting Information.

From Figure 4, it can be immediately noticed that the changes in electron population of the cycloether atoms are slighter than in the atoms of water molecule. In cycloethers, the atoms whose populations are affected when passing from the isolated state to the microhydrated complex formation (i.e., the absolute difference is greater than 0.02 *e*) are the carbon atoms adjacent to the heteroatom (C_2 and C_5 in THF; C_2 and C_6 in THP) which gain electrons (from 0.02 to 0.05 *e* in **nF** and **nP** complexes). This increase in electron population in the carbon atoms can be due to a possible consequence of the **P** H-bond formation, which substantially modifies the stereoelectronic effect produced by the heteroatom in the isolated cycloether.[24] Particularly, in complexes with the **HT** pattern, the hydrogen atoms involved in **S** H-bonds undergo a considerable loss in their atomic population (from −0.07 to −0.05 *e*) upon the complexation. For all analyzed complexes, the heteroatom experiences only a slight increase in its population with respect to that in the monomer. And in the case of **nF** and **nP** complexes with **HT** pattern, it can be noted that this atom (O_1) gradually gains electron density when *n* increase becomes $q(O_1)$ more negative.

In contraposition with the light changes observed in the cycloether atoms, the water molecule atoms directly involved in an H-bond experience a striking change in their population, upon complexation. The H_w atoms lose electrons ($\Delta N(H_w) < 0$) and the O_w atoms gain electrons ($\Delta N(O_w) > 0$) after creating either **P** or **B** H-bonds. Because of the gain in electron population in the O_w atoms, this leads to a negative charge of a larger magnitude than the positive charge of its attached H_w atoms. The positive/negative charge in the H_w/O_w atoms experiences a gradually slight increase in the **nF** and **nP** complexes with **HT** pattern when *n* increases. In this sense, the charges of the H_{w1}/O_{w1} atoms are +0.595/−1.156, +0.614/−1.171, +0.622/−1.184, and +0.624/−1.185 au for **1F−a**, **2F−a**, **3F−a**, and **4F−d**, respectively, and the same tendency is also found for the **nP** complexes with **HT** H-bonding pattern. In the **3F−c**, **4F−a** and **3P−b**, **4P−a** complexes the charge of the O_{w1} (−1.204, −1.224, −1.192, and −1.218 au, respectively) is more negative than in the correspondent complexes with **HT** pattern, because in the former complexes, the $H_2O_{(1)}$ molecule acts as double proton donor, with a considerable amount of electron population loss in its hydrogen atoms. (see Tables S4 and S5 of the Supporting Information).

In all analyzed complexes, the cycloether group loses electron population ($\sum\Delta N(\text{THF})$ and $\sum\Delta N(\text{THP}) < 0$). This electron population is transferred to the water molecules in the microhydrated complexes. In **1F−a** and **1P−a** complexes a charge transference of 0.026 *e* from each cycloether to $H_2O_{(1)}$ molecule occurs. This result is in line with the transference of charge density from a base to an acid (i.e., Koch and Popelier[44] have reported that in the systems $N_2\cdots HF$ and $NH_3\cdots HF$ occurs a transference of 0.005 and 0.046 *e*, respectively). In **nF** and **nP** complexes (n = 2−4) with **HT** pattern the cycloether group loses electron population (between 0.03 to 0.04 *e*), which is transferred, in the first place, to the $H_2O_{(1)}$ group through the $\mathbf{P_1}$ H-bond. However, the increase of population in $H_2O_{(1)}$ group is very small, null or even in certain cases, it loses electron population. In contraposition, the water molecule that interacts with the hydrophobic portion of the cycloether forming **S** H-bond, gains most of the transferred charge (between 80 to 90%). Thus, these results indicate that in the tri and tetrahydrated complexes with **HT** pattern, a concerted charge transference from cycloether to the water molecule involved in the **S** H-bond occurs through the intermediary water molecules linked by **B** H-bond. Thus, the $H_2O_{(2)}$ molecule in **2F−a** and **2P−a** complexes, the $H_2O_{(3)}$ molecule in **3F−a** and **3P−a** complexes and the $H_2O_{(4)}$ molecule in **4F−d** and **4P−d** complexes, are behaving as the end acceptor of electron population in a concerted charge transference chain.

In the **nF** and **nP** complexes (n = 3, 4) with **CL** pattern the electron population loss of the THF and THP groups range from −0.028 to −0.026 *e*, which is lower than that in the complexes with **HT** pattern. In these complexes with a **CL** pattern, the charge is transferred to the water molecules, too. However, it is also important to note that the charge is approximately and uniformly spread among water molecules, and as a result, each water group carries a null or slight positive charge with a magnitude ranging from 0.000 to +0.016 au. These results agree with the charge distribution of the water molecules in cluster and hydrated amino acid systems.[54] In summary, the results show that the supramolecular electron distribution undergoes considerable changes due to the addition of successive water molecules. It can be seen, mainly

dx.doi.org/10.1021/jp301498n | J. Phys. Chem. A 2012, 116, 4199−4210

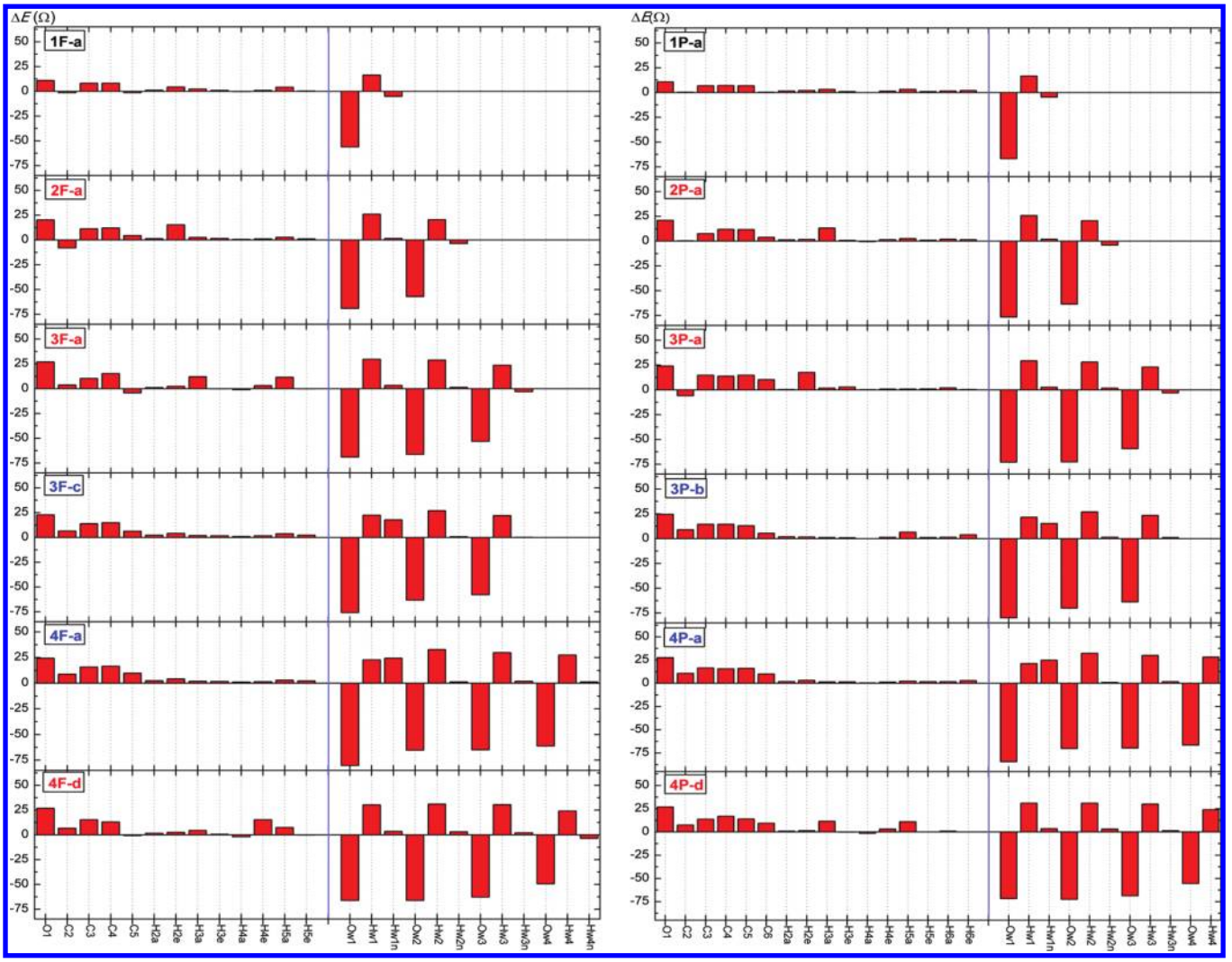

Figure 6. Variation of energy for all atoms of the selected **nF** (left) and **nP** (right) complexes in kcal/mol. The blue vertical line separates each bar graph into two regions: the one on the left corresponds to the cycloether atoms (THF and THP), and the other one corresponds to the water molecules atoms. $\Delta E(\Omega) < 0$ and $\Delta E(\Omega) > 0$ indicate that the atom is stabilized and destabilized upon the complexation, respectively. The complexes with **HT** and **CL** patterns are labeled in red and blue fonts, respectively. See Figures 1 and 2 to identify the complexes and atoms label. In the cases of H_{1-4wn} atoms, it indicate the hydrogen atom nonbonding in the H-bond except for complexes **3F−c**, **4F−a**, **3P−b**, and **4P−a**, where both hydrogen atoms of $H_2O_{(1)}$ form an H-bond.

in the water molecules subcluster that the charge gained by the oxygen atom is really noticeable and due to these findings, the hydrophobic hydration is viable. On the other hand, scarce change in the electron charge distribution is observed on the cycloether group in **CL** pattern complexes.

Energy Changes upon the Complexation. The energy of an atom in a molecule is well−defined within AIM theory through the application of the atomic statement of the virial theorem.[29] Figure 6 displays the variation in atomic energies of all atoms as a result of **nF** and **nP** complexes formation. Table 3 shows the sum of the $\Delta E(\Omega)$ of the atoms constituting the molecular groups ($\Sigma\Delta E(\Omega)$) for **nF** and **nP** complexes, respectively.

When analyzing the cycloether group, the heteroatom O_1, the hydrogen atoms involved in a H-bond and the carbon atoms adjacent to the heteroatom show a noticeable change in their atomic energy (greater than 10 kcal/mol in magnitude[52b]) upon the complexation. Overall, most atoms of both cycloether THF and THP experience a slight destabilization upon the formation of complexes. As a consequence, the sum of the changes in atomic energy of these atoms is positive ($\Sigma E(\mathrm{THF}) > 0$ and $\Sigma E(\mathrm{THP}) > 0$), and its magnitude increases gradually with the number of water molecules (see Table 3). It is also

Table 3. Change in Energy Summed up into Groups, $\sum\Delta E(\Omega)$ (in kcal/mol), for Selected nF and nP Complexes

complexes	cycloether	$H_2O_{(1)}$	$H_2O_{(2)}$	$H_2O_{(3)}$	$H_2O_{(4)}$
1F−a	38.21	−44.96			
2F−a	66.08	−41.54	−40.22		
3F−a	79.98	−35.93	−36.11	−32.93	
3F−c	82.54	−35.53	−35.62	−35.67	
4F−a	92.81	−33.20	−31.31	−32.26	−32.32
4F−d	90.30	−32.38	−32.13	−30.43	−28.93
1P−a	48.30	−54.81			
2P−a	81.10	−48.92	−46.89		
3P−a	99.05	−40.86	−43.06	−39.82	
3P−b	100.79	−43.00	−41.85	−39.50	
4P−a	114.46	−38.47	−37.09	−37.84	−37.34
4P−d	115.40	−37.02	−38.40	−37.15	−35.58

dx.doi.org/10.1021/jp301498n | J. Phys. Chem. A 2012, 116, 4199−4210

noticeable that the energetic change of the THP group is higher than in the THF group (the values of ΣE(THF) range from 38.21 to 92.81 kcal/mol and the values of ΣE(THP) values range from 48.30 to 115.40 kcal/mol).

In the water groups, the total energy changes are 44.96, 81.76, 104.97, 106.82, 129.09, and 123.87 kcal/mol for **1F−a**, **2F−a**, **3F−a**, **3F−c**, **4F−a**, and **4F−d**, complexes, respectively. The stabilization of water groups is supported by the considerable stabilization on O_w atoms. Particularly, in complexes with **CL** pattern, the O_{w1} atom experiences the most energetic stabilization. This stabilization is accompanied by the destabilization of the two hydrogen atoms of the $H_2O_{(1)}$ group. However, in the tri and tetrahydrated complexes that exhibit **CL** pattern the total stabilization of water groups is higher than in complexes with **HT** pattern. Thus, the major stabilization in the tetrahydrated complexes with **CL** H-bonding pattern (**4F−a** and **4P−a**) is supported by the additional gain of energetic stabilization of water groups. In all cases, the result of the net balance of the energetic destabilization cycloether group is surpassed by the total stabilization of the oxygen atoms of water groups.

4. CONCLUSIONS

In this work, the geometries, energies, and electronic properties of the THF/$(H_2O)_n$ and THF/$(H_2O)_n$ complexes (n = 1−4) have been systematically investigated to understand the role of **P**, **S**, and **B** H-bonds in the stabilization of microhydration structures and to find the H-bonding patterns involved. An AIM analysis has also been applied to know the distribution of the charge density and to pinpoint the atoms or region that experience electronic and energetic changes upon the complexation.

For the energetically most favorable microhydrated structures, two different H-bonding patterns were found. In one of them (**HT** pattern), a chain of water molecules engaged by **B** H-bonds is simultaneously bonded to the hydrophilic and hydrophobic portion of the cycloether, and in the other one (**CL** pattern), the water molecules are self-associated, forming a closed loop and one of them ($(H_2O)_1$ molecule) also forms a **P** H-bond with hydrophilic portion of the cycloether.

A linear correlation was established between the sum of electron density at all H-bond BCPs and the interaction energy (ΔE) as well as between the sum of electron density at the **P** and **S** H-bonds BCPs and the interaction energy solute−solvent (ΔE_{s-w}). The energetic analysis revealed that the major contributions to the ΔE of these mono- and dihydrated complexes come from c−w interactions, that is to say, from **P** and **S** H-bonds, but mainly from the former. A competition between c−w and w−w contribution was observed for trihydrated complexes. For most of tetrahydrated complexes, the **B** H-bonds provide the greatest contribution to the ΔE, whereas the contributions of **P** and **S** H-bonds are small but not negligible. Thus, the w−w interactions become more significant when the water molecules increase. Additionally, we have proposed a new way to estimate the contribution of different H-bonds to the stability of the system, based completely on charge density calculated at the H-bonds BCPs. In effect, we have found a reasonable agreement between the values of the $\mathcal{H}$ ratio proposed by Geronimo et al.[38] and the percentual contribution of the **B** H-bonds (B%) to the energy of the complexes. Even more, it allowed us to differentiate the contributions from solute−solvent interactions, in both hydrophilic (P%) and hydrophobic (S%) contributions. This is a promising feature, particularly to understand the organic compounds hydration applicable to large biological molecules.

From analysis of atomic and molecular group properties, we found that a charge transfer from cycloether to water molecules occurs in the microhydrated complexes. In complexes with **HT** pattern, the electron populations of the n^{th} water molecule increases considerably because it acts as the end electron acceptor in the chain of concerted charge transference. In contraposition, in complexes with a **CL** pattern, the electron population released by the cycloether is more evenly redistributed between each water molecule. Upon the complexation, the cycloether experiences an energetic destabilization that is counteracted by the remarkable energy stabilization experienced by the water molecules, as a consequence of the most energetic stabilization produced on their oxygen atoms.

Finally, we expect that while it is understood that the results pertain directly only to the model systems under scrutiny, they may help to understand better the hydration of more intricate systems as the amphiphilic biomolecules.

■ ASSOCIATED CONTENT

Supporting Information

Full citation of ref 43; figures show the optimized structures, and tables contain the optimized structural parameter, local topological properties of charge density at H-bond BCP, and atomic charge for microhydrated complexes. This material is available free of charge via the Internet at http://pubs.acs.org.

■ AUTHOR INFORMATION

Corresponding Author

*E-mail: arabeshai@yahoo.com.ar.

Notes

The authors declare no competing financial interest.

■ ACKNOWLEDGMENTS

We acknowledge SECYT−UNNE for financial support. M.M.V. is a fellow researcher of CONICET−UNNE, and N.M.P. is a career researcher of CONICET, Argentina. This work was supported by the Grants PICTO−UNNE 089 and PIP 095 CONICET.

■ REFERENCES

(1) Garczarek, F.; Gerwert, K. *Nature* **2006**, *439*, 109.
(2) Gertner, B. J.; Whitnell, R. M.; Wilson, K. R.; Hynes, J. T. *J. Am. Chem. Soc.* **1991**, *113*, 74.
(3) Maréchal, Y. *The Hydrogen Bond and the Water Molecule. The Physics and Chemistry of Water, Aqueous and Bio Media*; Elsevier: Amsterdam, Oxford, 2007.
(4) Ball, P. *Chem. Rev.* **2008**, *108*, 74.
(5) Elsaesser, T. *Acc. Chem. Res.* **2009**, *42*, 1220.
(6) Vaida, V. *J. Chem. Phys.* **2011**, *135*, 020901.
(7) Jeffrey, G. A. *An Introduction to Hydrogen Bonding*; Oxford University Press: Oxford, 1997.
(8) Desiraju, G. R.; Steiner, T. *The Weak Hydrogen Bond in Structural Chemistry and Biology*; Oxford University Press: New York, 1999.
(9) Sheiner, S. *Hydrogen Bonding*; Oxford University Press: NewYork, 1997.
(10) Grabowski, S. J. *Hydrogen Bondings: New Insights*; Springer: Berlin, 2006.
(11) Huang, Z.; Dai, Y.; Wang, H.; Yu, L. *J. Mol. Model.* **2011**, 1.
(12) (a) Pu, L.; Sun, Y.; Zhang, Z. *J. Phys. Chem. A* **2010**, *114*, 10842. (b) Pu, L.; Sun, Y.; Zhang, Z. *J. Phys. Chem. A* **2009**, *113*, 6841.
(13) (a) Gomide Freitas, L. C.; Marques Cordeiro, J. M. *J. Mol. Struct.: THEOCHEM* **1995**, *335*, 189. (b) Mrázková, E.; Hobza, P. *J.*

Phys. Chem. A **2003**, *107*, 1032. (c) Kulkarni, A. D.; Babu, K.; Gadre, S. R.; Bartolotti, L. J. *J. Phys. Chem. A.* **2004**, *108*, 2492.
(14) Lamsabhi, A. M. *J. Phys. Chem. A* **2008**, *112*, 1791.
(15) Sosa, G. L.; Peruchena, N. M.; Contreras, R.; Castro, E. A. *J. Mol. Struct.: THEOCHEM* **2002**, *577*, 219.
(16) (a) Takamuku, T.; Nakamizo, A.; Tabata, M.; Yoshida, K.; Yamaguchi, T.; Otomo, T. *J. Mol. Liq.* **2003**, *103*−*104*, 143. (b) Takamuku, T.; Tanaka, M.; Sako, T.; Shimomura, T.; Fujii, K.; Kanzaki, R.; Takeuchi, M. *J. Phys. Chem. B* **2010**, *114*, 4252.
(17) Katayama, M.; Ozutsumi, K. *J. Solution Chem.* **2008**, *37*, 841.
(18) Conrad, H.; Lehmkühler, F.; Sternemann, C.; Sakko, A.; Paschek, D.; Simonelli, L.; Huotari, S.; Feroughi, O.; Tolan, M.; Hämäläinen, K. *Phys. Rev. Lett.* **2009**, *103*, 218301.
(19) (a) Mizuno, K.; Miyashita, Y.; Shindo, Y.; Ogawa, H. *J. Phys. Chem.* **1995**, *99*, 3225. (b) Mizuno, K.; Kimurab, Y.; Morichika, H.; Nishimura, Y.; Shimada, S.; Maeda, S.; Imafuji, S.; Ochi, T. *J. Mol. Liq.* **2000**, *85*, 139.
(20) Oliveira, B. G.; Vasconcellos, M. L. A. A. *J. Mol. Struct.: THEOCHEM* **2006**, *74*, 83.
(21) Li, Q.; An, X.; Gong, B.; Cheng, J. *Spectrochim. Acta, Part A* **2008**, *69*, 211.
(22) Gojło, E.; Gampe, T.; Krakowiak, J.; Stangret, J. *J. Phys. Chem. A* **2007**, *111*, 1827.
(23) Mizuno, K.; Imafuji, S.; Fujiwara, T.; Ohta, T.; Tamiya, Y. *J. Phys. Chem. B* **2003**, *107*, 3972.
(24) Mizuno, K.; Masuda, Y.; Yamamura, T.; Kitamura, J.; Ogata, H.; Bako, I.; Tamai, Y.; Yagasaki, T. *J. Phys. Chem. B* **2009**, *113*, 906.
(25) Blanco, S.; López, J. C.; Lesarri, A.; Alonso, J. L. *J. Am. Chem. Soc.* **2006**, *128*, 12111 and references therein..
(26) Yang, C.; Li, W.; Wu, C. *J. Phys. Chem. B* **2004**, *108*, 11866.
(27) Stangret, J.; Gampe, T. *J. Mol. Struct.* **2005**, *734*, 183.
(28) Alavi, S.; Susilo, R.; Ripmeester, J. A. *J. Chem. Phys.* **2009**, *130*, 174501.
(29) Bader, R. F. W. *Atoms in Molecules: A Quantum Theory*; Oxford University Press: Oxford, U.K., 1990.
(30) Matta, C. F., Boyd, R. J., Eds. *The Quantum Theory of Atoms in Molecules: From Solid State to DNA and Drug Design*; Wiley-VCH: Weinheim, 2007.
(31) Hernandez, M. Z. *AGOA Program*, version 2.0; Depto. de Ciências Farmacêuticas (UFPE): Recife, Pernambuco, Brazil, 2003; http://www.ufpe.br/farmacia/zaldini/agoa.html.
(32) Vasconcellos, M. L. A. A.; Oliveira, B. G.; Leite, L. F. C. C. *J. Mol. Struct.: THEOCHEM* **2008**, *860*, 13.
(33) González, L.; Mó, O.; Yáñez, M.; Elguero, J. *J. Mol. Struct.: THEOCHEM* **1996**, *371*, 1.
(34) Boyd, S. L.; Boyd, R. J. *J. Chem. Theory Comput.* **2006**, *3*, 54.
(35) Becke, A. D. *J. Chem. Phys.* **1993**, *98*, 5648.
(36) Lee, C.; Yang, W.; Parr, R. G. *Phys. Rev. B* **1998**, *37*, 785.
(37) Pathak, A. K.; Mukherjee, T.; Maity, D. K. *J. Chem. Phys.* **2007**, *126*, 034301.
(38) Geronimo, I.; Chéron, N.; Fleurat−Lessard, P.; Dumont, É. *Chem. Phys. Lett.* **2009**, *481*, 173.
(39) Møller, C.; Plesset, M. S. *Phys. Rev.* **1934**, *46*, 618.
(40) Boys, S. F.; Bernardi, F. *Mol. Phys.* **1970**, *19*, 553.
(41) Biegler−König, F.; Schönbohn, J. *AIM2000*, Program Package version; Buöro fur Innovative Software Streibel Biegler− König Bielefel: Germany, 2002 (chemical advise by Bader, R. F. W. McMaster University: Hamilton, Canada, 2002).
(42) Biegler−König, F. *J. Comput. Chem.* **2000**, *21*, 1040.
(43) Frisch, M. J.; et al. *Gaussian 03*, Revision D.01; Gaussian, Inc.: Wallingford, CT, 2004.
(44) Koch, U.; Popelier, P. L. A. *J. Phys. Chem.* **1995**, *99*, 9747.
(45) (a) Sahu, P. K.; Lee, S.−L. *J. Chem. Phys.* **2005**, *123*, 044308. (b) Sahu, P. K.; Chaudhari, A.; Lee, S.−L. *Chem. Phys. Lett.* **2004**, *386*, 351.
(46) Vallejos, M. M.; Angelina, E. L.; Peruchena, N. M. *J. Phys. Chem. A* **2010**, *114*, 2855.
(47) Bowron, D. T.; Finney, J. L.; Soper, A. K. *J. Am. Chem. Soc.* **2006**, *128*, 5119.
(48) Bachrach, S. M. *J. Phys. Chem. A* **2008**, *112*, 3722.
(49) Tian, S. X. *J. Phys. Chem. B* **2004**, *108*, 20388.
(50) (a) Parthasarathi, R.; Subramanian, V.; Sathyamurthy, N. *J. Phys. Chem. A* **2005**, *109*, 843. (b) Parthasarathi, R.; Elango, M.; Subramanian, V.; Sathyamurthy, N. *J. Phys. Chem. A* **2009**, *113*, 3744.
(51) Mandal, A.; Prakash, M.; Kumar, R. M.; Parthasarathi, R.; Subramanian, V. *J. Phys. Chem. A* **2010**, *114*, 2250.
(52) (a) Matta, C. F.; Arabi, A. A.; Keith, T. A. *J. Phys. Chem. A* **2007**, *111*, 8864. (b) Arabi, A. A.; Matta, C. F. *J. Phys. Chem. A* **2009**, *113*, 3360.
(53) (a) Gonzalez Moa, M. J.; Mandado, M.; Mosquera, R. A. *Chem. Phys. Lett.* **2006**, *424*, 17. (b) Estévez, L.; Mosquera, R. A. *Chem. Phys. Lett.* **2008**, *451*, 121−26. (c) Estévez, L.; Mosquera, R. A. *J. Phys. Chem. A* **2009**, *113*, 9908.
(54) Devereux, M.; Popelier, P. L. A. *J. Phys. Chem. A* **2007**, *111*, 1536.